Eur. J. Mineral.
PrePub DOI: 10.1127/ejm/2015/0027-2445

PrePub Article

Crystal chemistry of cation-exchanged forms of epistolite-group minerals, Part I. Ag- and Cu-exchanged lomonosovite and Ag-exchanged murmanite

INNA S. LYKOVA[1,*], IGOR V. PEKOV[1], NATALIA V. ZUBKOVA[1], NIKITA V. CHUKANOV[2], VASILIY O. YAPASKURT[1], NADEZHDA A. CHERVONNAYA[2] and ANDREY A. ZOLOTAREV[3]

[1] Faculty of Geology, Moscow State University, Vorobievy Gory, 119991 Moscow, Russia
*Corresponding author, e-mail: innalykova@mail.ru
[2] Institute of Problems of Chemical Physics RAS, Chernogolovka, Moscow Region 142432, Russia
[3] Department of Crystallography, St. Petersburg State University, University Emb. 7/9, 199034 St. Petersburg, Russia

Abstract: The paper presents the first data on the crystal chemistry of the cation-exchanged forms of layered titanosilicates belonging to the epistolite group. It was found that these heterophyllosilicates have high exchange capacity and selectivity for cations of chalcophile elements (Ag, Cu and Zn) and could be considered as potentially novel raw materials or, more likely, as possible prototypes of cation-selective synthetic microporous materials. The crystal structures of Ag- and Cu-exchanged forms of lomonosovite and Ag-exchanged form of murmanite were studied by single-crystal X-ray diffraction. The topology of the main structural unit, the *HOH* block, remains unchanged in cation-exchanged forms as compared to the initial lomonosovite $Na_4Ti_4(Si_2O_7)_2O_4 \cdot 2Na_3PO_4$ (*P*-1) and murmanite $Na_4Ti_4(Si_2O_7)_2O_4 \cdot 4H_2O$ (*P*-1). In Ag-exchanged murmanite, Ag cations occupy two crystallographically non-equivalent positions: one in the heteropolyhedral (*H*) sheet and another one in the octahedral (*O*) sheet corresponding to the positions of Na in initial murmanite. The crystal structure of the Ag-exchanged form of lomonosovite is characterized by an increased unit-cell parameter *c* and doubled parameter *b* as compared to initial lomonosovite. Ten large-cation sites statistically occupied by Ag and Na correspond to the Na sites in the initial lomonosovite: six in the interlayer space, two in the *H* sheet and two in the *O* sheet. Silver significantly replaces Na in sites in the interlayer space and in the *O* sheet, whereas sites in the *H* sheet are less affected by the ion exchange. Unit-cell parameter *c* of the Cu-exchanged form of lomonosovite decreases by 3.58 % as compared to the initial lomonosovite whereas *a* and *b* remain almost the same. The Cu cations occupy two crystallographically independent positions. The Cu(1) site, corresponding to the Na(3) site in the initial lomonosovite, is located in the interlayer space. The low-occupancy Cu(2) site is located on the inversion centre in the *O* sheet; this site is vacant in the initial lomonosovite. The Cu(2) site is surrounded by six O atoms forming an octahedron distorted due to the Jahn-Teller effect.

Key-words: lomonosovite; murmanite; heterophyllosilicate minerals; layered titanosilicate; microporous material; ion exchange; crystal structure.

Introduction

The ion-exchange properties of various natural microporous titano-, niobo- and zirconosilicates with structures based on zeolite-like heteropolyhedral frameworks have been actively studied during the last two decades, including the ion-exchange capacity, kinetic and crystal chemistry of their cation-exchanged forms. The obtained results found applications in both the industry and the geosciences (see, *e.g.*, the reviews by Chukanov & Pekov, 2005, and Pekov & Chukanov, 2005). However, data on the layered titano- and niobosilicates as ion exchangers have not been reported until recently. Our studies show that heterophyllosillicate minerals belonging to the epistolite group prove to be the first known family of minerals that show strong affinity and selectivity in cation-exchange processes for chalcophile elements, including industrially important ones, whereas other, earlier studied silicate minerals demonstrated exchange selectivity to lithophile elements, in first place alkali and earth-alkali metals. Thus, these epistolite-group heterophyllosilicates could be considered as potentially novel raw materials or, more likely, as possible prototypes of cation-selective synthetic microporous materials.

Murmanite, ideally $Na_4Ti_4(Si_2O_7)_2O_4 \cdot 4H_2O$, and lomonosovite, $Na_4Ti_4(Si_2O_7)_2O_4 \cdot 2Na_3PO_4$, are layered titanosilicates (heterophyllosilicates) of the bafertisite mero-plesiotype series (Ferraris & Gula, 2005). Their crystal structures are based on the heterophyllosilicate *HOH* block. The central *O* sheet is composed by close-packed Na- and Ti-centred octahedra and is sandwiched between two *H* sheets consisting of alternating $[Si_2O_7]$ groups, Ti-centred octahedra and

DOI: 10.1127/ejm/2015/0027-2445

0935-1221/15/0027-2445 $ 6.75

Na-centred eight-fold polyhedra. The interlayer space contains Na^+ cations and PO_4^{3-} groups in lomonosovite or H_2O molecules in murmanite (Belov *et al.*, 1977; Khalilov, 1989).

Murmanite was briefly described by Ramsay (1890) as an ''unknown mineral #3'' from the Lovozero alkaline massif, Kola Peninsula, Russia, and later characterized as a new mineral species by Gutkova (1930). Lomonosovite was discovered at Lovozero by Gerasimovsky (1945, 1950). The morphological and chemical similarities of these minerals were obvious, and Borneman-Starynkevich (1946) showed that Na^+ and PO_4^{3-} can easily be leached from the interlayer space of lomonosovite and replaced by H_2O molecules which results in its transformation to murmanite.

The crystal structures of murmanite and lomonosovite were first examined by Khalilov *et al.* (1965) and repeatedly refined later (Rastsvetaeva *et al.*, 1971; Belov *et al.*, 1977; Rastsvetaeva & Andrianov, 1986; Khalilov, 1989; Nemeth *et al.*, 2005; Cámara *et al.*, 2008). The history of these studies is given in detail by Cámara *et al.* (2008).

Murmanite and lomonosovite are common accessories, and, sometimes, the rock-forming minerals of specific peralkaline rocks and their pegmatites (Khomyakov, 1995). Despite the wide distribution of these minerals, the long history of their studies and the many experiments on the transformation of lomonosovite into murmanite, the ion-exchange properties of these heterophyllosilicates have not been examined until recently. Only Selivanova (2012) briefly reported the ion exchange for murmanite in KCl solutions at room temperature: its K-exchanged form with 5.3–7.3 wt.% K_2O was obtained but no more data were published. We conducted the first systematic ion-exchange experiments with murmanite and lomonosovite in aqueous solutions of K, Rb, Cs, Ag, Sr, Cu^{2+}, Ni^{2+}, and Zn salts and found that both minerals have high exchange capacity and selectivity for cations of some chalcophile elements, namely Ag, Cu and Zn (Lykova *et al.*, 2013a and b).

In this paper we report the crystal-chemical data on the Ag- and Cu-exchanged forms of lomonosovite and the Ag-exchanged form of murmanite in comparison with the initial samples used for the ion-exchange experiments. The crystal chemistry of the Zn-exchanged forms of these heterophyllosilicates will be given, in comparison with natural zinc members of the epistolite group, in the companion paper, Part 2.

Experimental procedure

Analytical methods

The chemical composition of initial samples of murmanite and lomonosovite and their cation-exchanged forms was studied with a Jeol JSM-6480LV scanning electron microscope equipped with an energy dispersive X-ray spectrometer (EDS) INCA Energy-350 under the following conditions: operating voltage 25 kV, beam current 0.56 nA. The following standards were used: lorenzenite (Na$K\alpha$, Si$K\alpha$, Ti$K\alpha$), diopside (Ca$K\alpha$, Mg$K\alpha$), sanidine (K$K\alpha$), $AlPO_4$ (Al$K\alpha$, P$K\alpha$), $Cs_2Nb_4O_{11}$ (Nb$L\alpha$), $MnCO_3$ (Mn$K\alpha$), FeS_2 (Fe$K\alpha$), Cu_3VS_4 (Cu$K\alpha$). and Ag_2Se (Ag$L\alpha$). Iron and manganese oxidation states and H_2O content were not determined directly.

The X-ray diffraction studies were carried out using single-crystal diffraction data collected for more than a hemisphere of the reciprocal space on a Bruker Kappa APEX II diffractometer equipped with a CCD detector for lomonosovite and murmanite and in a full sphere of the reciprocal space on a Bruker Kappa APEX DUO diffractometer equipped with a CCD detector for Ag- and Cu-exchanged forms of lomonosovite and Ag-exchanged form of murmanite. The measured intensities were corrected for Lorentz, background, polarization and absorption effects.

The infrared absorption spectra were obtained using a Bruker Optics ALPHA FTIR spectrometer. The conditions were as follows: the wavenumber range from 360 to 3800 cm^{-1}, the resolution of 4 cm^{-1}, the number of scans of 16. Powdered minerals were mixed with dry KBr and pelletized. The IR spectrum of an analogous pure KBr disk was subtracted from the overall spectrum.

Initial samples and cation-exchange experiments

Murmanite samples for our experiments originate from a hydrothermally altered peralkaline pegmatite at Severnyi (North) open pit, Umbozero mine, Mt. Alluaiv, Lovozero alkaline complex. Lomonosovite samples were collected from the huge unaltered peralkaline pegmatite Koashva-99 at Mt. Koashva, Khibiny alkaline complex (both Kola Peninsula, Russia). Murmanite forms lilac lamellar crystals up to 0.05 × 2.5 × 3 cm in the ussingite–microcline zone of a pegmatite. Lomonosovite occurs as dark-brown to almost black tabular crystals up to 0.2 × 2 × 3.5 cm associated with aegirine, pectolite, villiaumite and thermonatrite.

The ion-exchange experiments with murmanite were performed in Teflon containers at room temperature, at 60°C and at 90°C (Lykova *et al.*, 2013a). As the experiment at 90°C showed the highest degree of exchange of Na for Ag, this sample was chosen for the crystal structure study. A portion of 5–10 mg of the mineral (fraction 0.5–2 mm) was placed in 15 ml of 1N aqueous $AgNO_3$ solution. Murmanite actively extracts silver from the solution with sodium displacement. The Ag-exchanged form of murmanite contains 3.3-3.7 Ag *apfu* (atoms per formula unit, henceforth calculated on the basis of 4 Si + Al), whereas the initial sodium content was 2.7–2.9 *apfu* (Table 1). The possible schemes of the exchange are discussed in detail below. The reaction spreads over the entire volume of a grain within several hours.

Lomonosovite did not show the ion-exchange properties for Ag or Cu at 90°C. For the experiments at 150°C, sealed glass ampoules were used. In the experiments with 1N aqueous $AgNO_3$ solution, a novel Ag-rich phase (up to 58.8 wt. % Ag_2O) was formed. The content of P (*apfu*) in this phase remains the same as in the initial lomonosovite

Table 1. Chemical composition of murmanite (Mur) and product of its reaction with $AgNO_3$ solution at 90°C (AgMur), lomonosovite (Lom) and products of its reactions with $AgNO_3$ (AgLom) and $CuSO_4$ (CuLom) solutions at 150°C.

			AgMur		AgLom		CuLom				
Reaction time	Lom	Mur	5 hours		3 days		5 hours	28 hours		7 days	
wt. %											
Na_2O	26.50	11.40	1.40	–	–	2.29	6.50	5.00	4.77	3.76	3.15
K_2O	–	0.50	–	–	–	–	–	–	–	–	–
Ag_2O	–	–	34.40	32.40	58.77	53.18	–	–	–	–	–
CaO	2.70	4.20	2.50	2.00	0.44	1.00	2.11	1.97	2.29	2.15	2.22
CuO	–	–	–	–	–	–	12.15	14.53	14.62	14.80	13.42
MgO	0.57	0.40	0.60	–	0.44	0.59	0.48	0.50	0.49	0.52	0.70
FeO	2.44	2.00	1.10	0.60	1.30	1.16	2.24	2.67	2.76	2.41	2.62
MnO	1.94	2.40	2.00	1.00	0.73	0.86	1.79	1.66	1.78	1.49	1.79
Al_2O_3	–	–	–	–	–	–	–	0.04	0.27	–	–
SiO_2	23.21	30.20	20.90	18.70	13.13	13.34	24.60	24.25	23.98	23.33	24.02
TiO_2	22.87	27.30	21.00	22.10	11.71	13.18	24.92	23.52	22.96	23.27	22.29
Nb_2O_5	4.28	5.90	3.20	1.70	4.31	2.50	4.71	5.23	5.17	3.99	4.57
P_2O_5	13.49	1.60	–	–	7.52	7.82	14.02	14.33	14.38	13.61	13.65
Total	98.00	85.90	87.20	78.60	98.36	95.92	93.52	93.70	93.47	89.33	88.44
Atoms per formula unit (based on Si+Al = 4)											
Na	8.86	2.90	0.52	–	–	1.33	2.05	1.59	1.52	1.25	1.02
K	–	0.10	–	–	–	–	–	–	–	–	–
Ag	–	–	3.42	3.59	9.28	8.27	–	–	–	–	–
Ca	0.50	0.60	0.52	0.47	0.15	0.32	0.37	0.35	0.40	0.39	0.40
Cu	–	–	–	–			1.49	1.81	1.82	1.92	1.69
Mg	0.14	0.10	0.17	–	0.20	0.26	0.12	0.12	0.12	0.13	0.17
Fe	0.35	0.20	0.18	0.11	0.33	0.29	0.31	0.37	0.38	0.35	0.37
Mn	0.28	0.30	0.33	0.17	0.19	0.22	0.25	0.23	0.25	0.22	0.25
Al	–	–	–	–	–	–	–	0.01	0.05	–	–
Si	4.00	4.00	4.00	4.00	4.00	4.00	4.00	3.99	3.95	4.00	4.00
Ti	2.97	2.70	3.03	3.55	2.68	2.97	3.05	2.91	2.84	3.00	2.79
Nb	0.33	0.40	0.28	0.17	0.59	0.34	0.35	0.39	0.39	0.31	0.34
P	1.97	0.20	–	–	1.94	1.98	1.93	2.00	2.01	1.98	1.92

(Table 1). The replacement takes over 50–80 % of the grains volume within several days (Fig. 1), and then the exchange rate drops significantly.

The products, mechanism and kinetics of the ion-exchange reactions of murmanite and lomonosovite with Ag are discussed by Lykova *et al.* (2013b).

In the experiments with 1N aqueous $CuSO_4$ solution, a new phase with 1.5–1.9 *apfu* Cu develops within the first hours along the cleavage fractures of initial lomonosovite (Fig. 2a) and further spreads over the entire grains (Fig. 2b). The P content in this Cu-exchanged form of lomonosovite remains the same as in initial lomonosovite (Table 1). Unfortunately, the acidic character of the $CuSO_4$ solution causes partial dissolution of a thin peripheral zone of lomonosovite grains and damage (slight amorphization) of other products of the reaction. A rim of another phase, with higher Ti/Si ratio, is formed around lomonosovite grains (Fig. 2b).

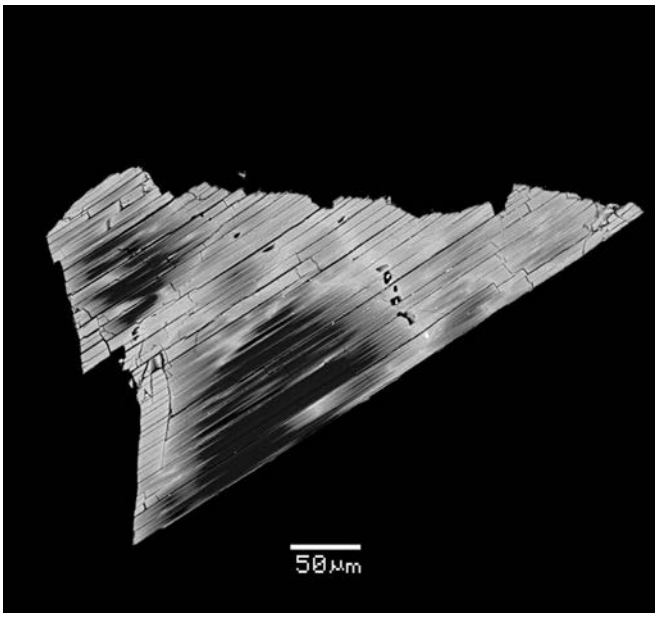

Fig. 1. Product of the reaction of lomonosovite with 1N $AgNO_3$ solution at 150°C during three days. Bright areas correspond to the Ag-exchanged form of lomonosovite, dark areas are relics of the initial mineral. Back-scattered electron (BSE) image.

Single-crystal X-ray diffraction

For single-crystal X-ray diffraction studies, products of the reactions with $AgNO_3$ solution (during 3 days for lomonosovite and 5 hours for murmanite) and with $CuSO_4$ solution

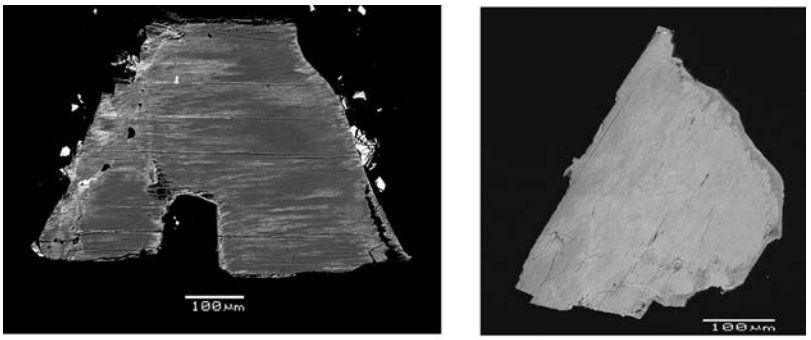

Fig. 2. Products of the reaction of lomonosovite with 1N $CuSO_4$ solution at 150°C during 5 (a) and 28 (b) hours. Bright areas correspond to the Cu-exchanged form of lomonosovite, dark areas (a) are relics of the initial mineral. SEM (BSE) images.

(during 28 hours for lomonosovite), *i.e.*, phases with a significant degree of exchange and minimum effects of amorphization and hydrolysis were used.

The crystal structures were solved by direct methods and refined by full-matrix least-squares techniques on F^2 in the space group *P*-1 using the SHELX-97 program package (Sheldrick, 2008). The crystal data, the details of the X-ray diffraction studies and the structure refinement parameters are given in Table 2, atom coordinates, equivalent displacement parameters, site occupancy factors or refined site-scatterings, bond-valence sum values (Brese & O'Keeffe, 1991) and selected interatomic distances in Tables 3–12.

The crystal structures of the initial murmanite and lomonosovite were refined to $R = 0.0665$ (1803 independent reflections with $I > 2\sigma(I)$) and to $R = 0.0251$ (2346 independent reflections with $I > 2\sigma(I)$) (Table 2). The Ag-exchanged form of murmanite was refined on the basis of 1907 independent reflections with $I > 2\sigma(I)$ to $R = 0.0658$. The data sets for the exchanged samples of lomonosovite are of lower quality due to uneven Ag and Cu distribution. Slight hydration during the experiments could also contribute to the diffracted intensities. The final *R* values are 12.28 % for Ag-exchanged lomonosovite and 12.58 % for Cu-exchanged lomonosovite, respectively.

Table 2. Crystal data, data collection information and structure refinement details for murmanite (Mur), its Ag-exchanged form (AgMur), lomonosovite (Lom) and its Ag- and Cu-exchanged forms (AgLom and CuLom respectively).

Sample	Mur	AgMur	Lom	AgLom	CuLom
Space group, Z	*P*-1, 1	*P*-1, 1	*P*-1, 1	*P*-1, 1	*P*-1, 1
a, Å	5.3741(6)	5.4043(3)	5.41160(10)	5.4071(5)	5.2653(19)
b, Å	7.0750(9)	7.1687(4)	7.1227(2)	14.2614(12)	7.153(3)
c, Å	12.1947(15)	12.2593(8)	14.4871(4)	14.6246(14)	13.969(5)
α	92.996(7)	92.723(4)	99.7395(16)	99.477(3)	100.050(9)
β	107.758(8)	107.881(4)	96.5470(16)	96.169(3)	96.829(9)
γ	90.100(8)	90.398(4)	90.2800(17)	90.355(3)	91.905(10)
V, Å^3	440.89(9)	451.38(5)	546.60(2)	1105.58(17)	513.6(3)
λ (Mo*K*α) (Å), *T* (K)			0.71073, 293(2)		
Diffractometer	Kappa APEX II CCD	Kappa APEX DUO CCD	Kappa APEX II CCD	Kappa APEX DUO CCD	Kappa APEX DUO CCD
Reflections collected	3871	11157	5266	14940	7773
Unique reflections, R_{int}	2151, 0.0350	2236, 0.0578	2702, 0.0220	5429, 0.0295	2083, 0.0564
Reflections with $I > 2\sigma(I)$	1803	1907	2346	4071	1727
Refinement on			F^2		
No. of refined parameters	158	159	216	391	206
*R*1	0.0665	0.0658	0.0251	0.1228	0.1258
w$R2_{all}(F^2)$	0.1747	0.1615	0.0606	0.2703	0.2992
GoF	1.0768	1.154	1.050	1.103	1.156
$\Delta\rho_{max}$ /$\Delta\rho_{min}$ (e/Å^3)	1.572/-0.916	2.383/-1.417	0.381/-0.554	3.282/-4.447	3.208/-1.672

Table 3. Atom coordinates (*x, y, z*), equivalent thermal displacement parameters (U_{eq}, Å^2), site occupancy factors (s.o.f.) and bond-valence sums (BVS) in the structure of murmanite.

Atom	*x*	*y*	*z*	U_{eq}	s.o.f.[1]	BVS[2]
Si(1)	0.9228(3)	0.0515(2)	0.26037(15)	0.0236(4)	1	4.02
Si(2)	0.9481(3)	0.6241(2)	0.27720(15)	0.0251(4)	1	4.22
Ti(1)	0.41430(18)	0.32665(14)	0.23755(10)	0.0271(4)	[24.0] $Ti_{0.89}Nb_{0.11}$	4.28
Ti(2)	0.2765(2)	0.88533(14)	0.50506(9)	0.0268(4)	[23.5] $Ti_{0.67}Mn_{0.30}Nb_{0.02}$	3.64
Na(1)	0.7332(7)	0.6090(5)	0.4895(3)	0.0413(14)	[9.2] 0.835(15)	0.91
Na(2)	0.3842(5)	0.8295(4)	0.2002(2)	0.0349(9)	[11.5] $Na_{0.50}Ca_{0.30}$	1.02
O(1)	0.5337(8)	0.2982(6)	0.3943(4)	0.0304(10)	1	2.01
O(2) = (O,OH)	0.5025(8)	0.8963(6)	0.4128(4)	0.0271(9)	1	1.71
O(3)	0.9015(11)	0.8250(6)	0.2178(4)	0.0405(12)	1	2.13
O(4)	0.0015(8)	0.9336(6)	0.5985(4)	0.0248(9)	1	1.86
O(5)	0.0606(9)	0.6675(6)	0.4161(4)	0.0326(10)	1	2.02
O(6)	0.1384(10)	0.1382(9)	0.2110(5)	0.0462(14)	1	1.94
O(7)	0.6372(10)	0.1336(8)	0.2021(5)	0.0463(14)	1	1.92
O(8)	0.1635(10)	0.5207(8)	0.2316(5)	0.0471(14)	1	1.99
O(9)	0.6703(11)	0.5219(9)	0.2416(5)	0.0493(15)	1	1.95
O(10) = H_2O	0.2837(12)	0.3450(8)	0.0462(5)	0.0485(13)	1	0.33
O(11) = H_2O	0.2509(12)	0.7276(10)	0.0060(6)	0.0603(17)	1	0.23

[1] Basing on the e_{ref} values (given in square brackets) and electron microprobe data we consider these occupancies of the sites, taking into account coordination polyhedra character and interatomic distances.
[2] BVS have been formally calculated taking into account s.o.f.

Table 4. Selected interatomic distances (Å) for murmanite.

Ti(1) - octahedron			Ti(2) - octahedron		
Ti(1)	-O(1)	1.844(5)	Ti(2)	-O(2)	1.895(4)
	-O(8)	1.914(5)		-O(1)	1.908(5)
	-O(6)	1.933(5)		-O(2)	1.977(4)
	-O(7)	1.936(5)		-O(5)	1.987(5)
	-O(9)	1.936(5)		-O(4)	2.120(4)
	-O(10)	2.233(6)		-O(4)	2.142(4)
<Ti(1)–O>		1.966	<Ti(2)–O>		2.005
Si(1) - tetrahedron			Si(2) - tetrahedron		
Si(1)	-O(6)	1.595(5)	Si(2)	-O(9)	1.584(5)
	-O(7)	1.606(5)		-O(8)	1.593(5)
	-O(4)	1.640(5)		-O(3)	1.614(5)
	-O(3)	1.651(5)		-O(5)	1.628(5)
<Si(1)–O>		1.623	<Si(2)–O>		1.605
Na(1) - octahedron			Na(2) - polyhedron		
Na(1)	- O(5)	2.250(6)	Na(2)	-O(11)	2.329(7)
	-O(1)	2.375(5)		-O(2)	2.493(5)
	-O(5)	2.417(6)		-O(7)	2.538(7)
	-O(2)	2.459(5)		-O(6)	2.573(7)
	-O(1)	2.510(6)		-O(8)	2.585(7)
	-O(4)	2.761(6)		-O(9)	2.647(7)
<Na(1)–O>		2.462		-O(3)	2.668(6)
				-O(3)	2.722(6)
			<Na(2)–O>		2.569

However, in spite of relatively high *R*, reasonable interatomic distances (Tables 10 and 12), atom displacement parameters and bond valence sums (Tables 9 and 11) show that the obtained structure models are correct.

Unfortunately all tested crystals of Cu-exchanged murmanite demonstrated a low quality that prevented the collection of data suitable for structure refinement.

Results and discussion

The main structural and topological features of lomonosovite and murmanite were discussed in the summarizing paper by Ferraris & Gula (2005). We focus on the structural comparison of initial lomonosovite and murmanite with their cation-exchanged forms.

Initial murmanite

There are two distorted octahedra centred by Ti(2) and Na(1) in a 1:1 ratio in the octahedral *O* sheet of the *HOH* block in the structure of initial murmanite (Fig. 3a). The Ti(2) site is Ti-dominant with 0.30 Mn and 0.02 Nb. The Na(1) site is occupied solely by Na with 84 % occupancy and *a* <Na(1) – O> distance of 2.46 Å (Tables 3–4). The composition of the heteropolyhedral *H* sheet corresponds to the simplified formula $[NaTiSi_2O_7]^-$. It consists of the tetrahedral disilicate groups Si_2O_7 alternating with Ti(1)-centred octahedra and Na(2)-centred eight-fold polyhedra. ''Pendent'' vertices of Ti(1)- and Na(2)-centred polyhedra [O(10) and O(11) respectively] are occupied by H_2O molecules. The Ti(1) site is occupied predominantly by Ti with admixture of heavy Nb (11 % of site occupancy). The Ti(1)-centred octahedron is distorted: five short interatomic Ti(1)–O distances vary from 1.844(5) to 1.936(5) Å whereas the sixth Ti(1)–O(10) bond is 2.233(6) Å long. The Na(2) site is occupied by 0.50 Na + 0.30 Ca + 0.20 □ with a refined number of electrons (e_{ref}) of 11.5 and an average <Na(2)–O> distance of 2.57 Å (Table 4). Thus both large cation sites in the initial murmanite contain vacancies. The most probable mechanism of charge compensation is partial protonation of the bridging oxygen in Ti(2)–O(2)–Ti(2). It is confirmed by bond-valence calculation for O(2) = 1.71 *vu* (valence units; Table 3) and the

Table 5. Atom coordinates (*x, y, z*), equivalent thermal displacement parameters (U_{eq}, Å^2), site occupancy factors (s.o.f.) and bond-valence sums (BVS) in the structure of Ag-exchanged form of murmanite.

Atom	*x*	*y*	*z*	U_{eq}	s.o.f.[1]	BVS[2]
Si(1)	0.9240(5)	0.0500(3)	0.2583(2)	0.0146(6)	1	3.94
Si(2)	0.9552(5)	0.6253(3)	0.2742(2)	0.0168(6)	1	4.02
Ti(1)	0.4210(3)	0.3270(2)	0.23604(15)	0.0177(5)	[24.4] $Ti_{0.88}Nb_{0.12}$	4.54
Ti(2)	0.2745(3)	0.8906(2)	0.50519(14)	0.0175(6)	[24.6] $Ti_{0.57}Mn_{0.35}Nb_{0.08}$	4.04
Ag(1)	0.72810(16)	0.60669(11)	0.49285(9)	0.0297(3)	[45.6] $Ag_{0.96}Na_{0.04}$	0.91
Ag(2)	0.3925(2)	0.83057(17)	0.19761(12)	0.0299(4)	[32.9] $Ag_{0.69}Ca_{0.25}Na_{0.06}$	1.09
O(1)	0.5437(13)	0.2942(10)	0.3905(6)	0.0234(15)	1	2.17
O(2)	0.4997(12)	0.8992(9)	0.4123(6)	0.0182(14)	1	1.92
O(3)	0.9044(14)	0.8287(9)	0.2135(6)	0.0253(16)	1	2.06
O(4)	0.0062(11)	0.9398(9)	0.6010(6)	0.0164(13)	1	1.96
O(5)	0.0611(13)	0.6725(10)	0.4133(6)	0.0225(15)	1	2.02
O(6)	0.1387(15)	0.1457(11)	0.2108(7)	0.0291(17)	1	1.94
O(7)	0.6389(14)	0.1309(11)	0.1995(7)	0.0279(17)	1	1.95
O(8)	0.1804(14)	0.5272(11)	0.2336(7)	0.0300(18)	1	1.99
O(9)	0.6846(14)	0.5120(12)	0.2360(7)	0.0319(19)	1	1.95
O(10) = H_2O	0.2807(17)	0.3413(12)	0.0443(8)	0.037(2)	1	0.35
O(11) = H_2O	0.247(2)	0.7176(19)	–0.0009(11)	0.069(4)	1	0.22

[1] Basing on the e_{ref} values (given in square brackets) and electron microprobe data we consider these occupancies of the sites, taking into account coordination polyhedra character and interatomic distances.
[2] BVS have been formally calculated taking into account s.o.f.

Table 6. Selected interatomic distances (Å) for the Ag-exchanged form of murmanite.

Ti(1) - octahedron			Ti(2) - octahedron		
Ti(1)	-O(1)	1.831(8)	Ti(2)	-O(2)	1.907(7)
	-O(6)	1.938(7)		-O(1)	1.940(7)
	-O(8)	1.939(7)		-O(2)	1.963(7)
	-O(9)	1.939(7)		-O(5)	2.013(7)
	-O(7)	1.962(7)		-O(4)	2.107(7)
	-O(10)	2.245(9)		-O(4)	2.149(6)
<Ti(1)–O>		1.976	<Ti(2)–O>		2.013
Si(1) - tetrahedron			Si(2) - tetrahedron		
Si(1)	-O(7)	1.612(7)	Si(2)	-O(9)	1.596(7)
	-O(6)	1.612(7)		-O(8)	1.604(7)
	-O(4)	1.646(7)		-O(5)	1.641(8)
	-O(3)	1.646(7)		-O(3)	1.655(8)
<Si(1)–O>		1.629	<Si(2)–O>		1.624
Ag(1) - octahedron			Ag(2) - polyhedron		
Ag(1)	-O(5)	2.350(7)	Ag(2)	-O(11)	2.414(14)
	-O(1)	2.432(7)		-O(7)	2.519(8)
	-O(5)	2.464(7)		-O(2)	2.538(7)
	-O(2)	2.525(7)		-O(8)	2.570(8)
	-O(1)	2.553(7)		-O(6)	2.675(8)
	-O(4)	2.854(6)		-O(3)	2.703(7)
<Ag(1)–O>		2.530		-O(3)	2.713(7)
				-O(9)	2.762(9)
			<Ag(2)–O>		2.61

presence of a weak shoulder at 3530 cm^{-1} in the IR spectrum of initial murmanite, corresponding to O-H stretching vibrations of basic OH groups (Fig. 4).

The formula of murmanite obtained from the structural refinement is $\{Na_{1.68}(Ti_{1.36}Mn_{0.60}Nb_{0.04})\}\{Na_{1.00}Ca_{0.60}(Ti_{1.78}Nb_{0.22})[Si_2O_7]_2\}O_2(O,OH)_2(H_2O)_4$ in which the contents of the *O* and *H* sheets are shown in braces.

Ag-exchanged murmanite

The crystal structure of the Ag-exchanged form of murmanite is characterized by slightly increased unit-cell parameters (Table 2) compared to the initial form, whereas the topology of the main structural *HOH* block remains unchanged. The Ag cations occupy two crystallographically non-equivalent positions Ag(1) and Ag(2): one in the *O* and another in the *H* sheet, corresponding to the positions of Na(1) and Na(2), respectively, in the initial murmanite (Fig. 3b). There are no Ag sites in the interlayer space. The Ag(1) site is Ag-dominant with a small admixture of Na (4 % of site occupancy). The Ag(2) site is occupied by 0.69 Ag + 0.25 Ca + 0.06 Na (e_{ref} = 32.9, Table 5). The exchange of Na for Ag results in an increase in size of both polyhedra: average distances in them are <Ag(1)–O> = 2.53 Å and <Ag(2)–O> = 2.61 Å (Table 6). Unlike the initial murmanite, both large-cation sites in its Ag-exchanged form are fully occupied. The Ag^+ ion actively replaces Na^+ and occupies also vacancies, whereas bivalent Ca is rigidly fixed in its site and remains inert during the reaction.

Thus, besides the ''classic'' exchange scheme $Na^+ \rightarrow Ag^+$, the two following ones can be hypothesized: $\square + OH^- \rightarrow Ag^+ + O^{2-}$ and/or $\square + H_2O \rightarrow Ag^+ + OH^-$. This is confirmed by the IR spectroscopy data and bond-valence calculations (Table 5). In the IR spectrum of the Ag-exchanged form of murmanite (Fig. 4) the shoulder at 3530 cm^{-1} corresponding to O-H stretching vibrations of

Table 7. Atom coordinates (*x, y, z*), equivalent thermal displacement parameters (U_{eq}, Å^2), site occupancy factors (s.o.f.) and bond-valence sums (BVS) in the structure of lomonosovite.

Atom	*x*	*y*	*z*	U_{eq}	s.o.f.[1]	BVS[2]
Si(1)	0.64867(11)	0.63898(8)	0.19827(4)	0.00775(13)	1	4.12
Si(2)	0.66524(11)	0.20257(8)	0.17705(4)	0.00806(13)	1	3.91
Ti(1)	0.16434(6)	0.92582(5)	0.21680(2)	0.00713(12)	[23.3] $Ti_{0.93}Nb_{0.07}$	4.35
Ti(2)	0.23049(7)	0.61282(5)	0.00733(2)	0.01129(12)	[24.3] $Ti_{0.67}Mn_{0.25}Nb_{0.08}$	3.75
P	0.17793(10)	0.22359(7)	0.43296(4)	0.01005(13)	1	4.74
Na(1)	0.75680(17)	0.88214(13)	–0.00408(7)	0.0242(2)	1	1.08
Na(2)	0.17170(18)	0.41494(13)	0.23406(6)	0.0192(2)	1	1.11
Na(3)	0.68054(15)	-0.02649(10)	0.35917(5)	0.0155(3)	[12.7] $Na_{0.70}Ca_{0.25}$	1.23
Na(4)	0.6760(2)	0.46015(14)	0.39794(7)	0.0231(2)	1	1.04
Na(5)	0.7634(2)	0.26184(13)	0.58609(7)	0.0236(2)	1	1.03
O(1)	0.1282(3)	0.8352(2)	0.09213(11)	0.0154(3)	1	2.16
O(2)	0.0892(3)	0.4227(2)	0.07048(10)	0.0134(3)	1	1.92
O(3)	0.6718(3)	0.4273(2)	0.23035(10)	0.0134(3)	1	2.21
O(4)	0.4051(3)	0.3919(2)	–0.08356(10)	0.0136(3)	1	1.93
O(5)	0.3600(3)	0.8051(2)	–0.06517(10)	0.0131(3)	1	2.08
O(6)	0.4157(3)	0.7336(2)	0.24935(10)	0.0119(3)	1	2.03
O(7)	–0.0950(3)	0.7506(2)	0.24569(11)	0.0139(3)	1	1.89
O(8)	0.4347(3)	0.1026(2)	0.21052(12)	0.0203(4)	1	2.02
O(9)	–0.0750(3)	0.1199(2)	0.21500(12)	0.0189(4)	1	2.17
O(10)	0.2342(3)	0.0337(2)	0.36764(11)	0.0152(3)	1	1.94
O(11)	0.3263(3)	0.2287(2)	0.53020(11)	0.0209(4)	1	1.93
O(12)	0.2518(3)	0.3981(2)	0.39171(11)	0.0186(4)	1	1.90
O(13)	–0.1006(3)	0.2248(2)	0.44241(12)	0.0187(4)	1	2.18

[1] Basing on the e_{ref} values (given in square brackets) and electron microprobe data we consider these occupancies of the sites, taking into account coordination polyhedra character and interatomic distances.
[2] BVS have been formally calculated taking into account s.o.f.

basic OH groups is stronger than that in the IR-spectrum of initial murmanite, whereas the bands in the range 3200–3400 cm^{-1} corresponding to more acidic OH groups and H_2O molecules became weaker after exchange with Ag. The bond-valence sum of the Ti(2)–O–Ti(2) bridge oxygen O(2) in the Ag-exchanged form of murmanite is higher (1.92 *vu*) than in the initial murmanite (1.71 *vu*), which indicates possible deprotonation of the OH^- groups.

The formula of the Ag-exchanged form of murmanite obtained from the structural refinement is $\{Ag_{1.92}Na_{0.08}(Ti_{1.14}Mn_{0.70}Nb_{0.16})\}\{Ag_{1.38}Ca_{0.50}Na_{0.12}(Ti_{1.76}Nb_{0.24})[Si_2O_7]_2\}O_4(H_2O,OH)_4$, in which the contents of the *O* and *H* sheets are shown in braces. It corresponds to the empirical formula calculated on the basis of electron-microprobe data (Table 1).

Initial lomonosovite

In the initial lomonosovite the *HOH* block is the same as in murmanite (Fig. 5). The Ti(1) site in the *H* sheet is occupied by 0.93 Ti + 0.07 Nb, and the Ti(2) site in the *O* sheet contains 0.67 Ti + 0.25 Mn + 0.08 Nb (e_{ref} = 24.3; Table 7). The large cation sites Na(1) (average distance <Na(1)–O> 2.47 Å) and Na(2) (<Na(2)–O> 2.57 Å; Table 8) are fully occupied by Na. There are three large cation sites in the interlayer space with different coordination numbers: six-fold Na(3)-centred polyhedron (<Na(3)–O> 2.45 Å), four-fold Na(4)-centred polyhedron (<Na(4)–O> 2.30 Å) and Na(5)-centred five-fold polyhedron (<Na(5)–O> 2.41 Å). The Na(4) and Na(5) sites are occupied solely by Na whereas Na(3) is Na-dominant with admixture of Ca (25 % of the site occupancy). One P site in the interlayer space is fully occupied; the average <P–O> distance in the PO_4 tetrahedron is 1.54 Å. There are 13 anion sites O(1–13), occupied by O atoms which have bond-valence sums of 1.89–2.21 *vu* (Table 7).

The lomonosovite formula obtained from the structural refinement is $\{Na_{3.40}Ca_{0.50}\}\{Na_{2.00}(Ti_{1.34}Mn_{0.50}Nb_{0.16})$[1]$\}\{Na_{2.00}(Ti_{1.86}Nb_{0.14})[Si_2O_7]_2\}(PO_4)_2O_4$, in which the contents of the interlayer space, *O* and *H* sheets are correspondingly given in braces.

Ag-exchanged lomonosovite

The Ag-exchanged form of lomonosovite is characterized by an increased *c* parameter and a doubled *b* parameter of the unit-cell as compared to the initial lomonosovite (Table 2). Yet the topology of the *HOH* block remains unchanged (Fig. 6a).

The crucial distinction from the initial lomonosovite is observed in the arrangement of PO_4 tetrahedra. The P(1)-centred tetrahedron is regular with an average <P–O> distance of 1.54 Å, whereas another P site is split along *a* into the two sub-sites P(2) and P(2'). The occupancies have

[1]This site can also contain minor admixture of Fe^{3+}.

Table 8. Selected interatomic distances (Å) for lomonosovite.

Ti(1) - octahedron			Ti(2) - octahedron		
Ti(1)	-O(1)	1.8001(15)	Ti(2)	-O(2)	1.9447(16)
	-O(9)	1.9003(16)		-O(2)	1.9556(15)
	-O(8)	1.9458(16)		-O(1)	1.9568(16)
	-O(7)	1.9990(16)		-O(5)	2.0287(16)
	-O(6)	2.0093(15)		-O(4)	2.1511(16)
	-O(10)	2.1794(15)		-O(4)	2.1677(15)
<Ti(1)–O>		1.972	<Ti(2)–O>		2.034
Si(1) - tetrahedron			Si(2) - tetrahedron		
Si(1)	-O(7)	1.6172(16)	Si(2)	-O(8)	1.5951(17)
	-O(6)	1.6258(15)		-O(9)	1.6022(16)
	-O(4)	1.6310(16)		-O(5)	1.6025(15)
	-O(3)	1.6525(15)		-O(3)	1.6536(15)
<Si(1)–O>		1.632	<Si(2)–O>		1.614
P - tetrahedron			Na(1) - octahedron		
P	-O(13)	1.5287(17)	Na(1)	- O(5)	2.2542(18)
	-O(11)	1.5347(17)		-O(1)	2.3706(19)
	-O(12)	1.5371(16)		-O(5)	2.4023(17)
	-O(10)	1.5665(15)		-O(2)	2.4143(17)
<P–O>		1.542		-O(1)	2.6659(19)
				-O(4)	2.6955(19)
			<Na(1)–O>		2.467
Na(2) - polyhedron			Na(3) - polyhedron		
Na(2)	-O(12)	2.2991(19)	Na(3)	-O(13)	2.2325(18)
	-O(2)	2.3710(17)		-O(11)	2.3324(19)
	-O(9)	2.4425(19)		-O(6)	2.4579(16)
	-O(6)	2.5844(18)		-O(10)	2.4683(18)
	-O(8)	2.6413(19)		-O(7)	2.5079(17)
	-O(3)	2.7015(18)		-O(8)	2.6983(19)
	-O(3)	2.7146(18)	<Na(3)–O>		2.450
	-O(7)	2.7895(18)			
<Na(2)–O>		2.568			
Na(4) - polyhedron			Na(5) - polyhedron		
Na(4)	- O(13)	2.2123(19)	Na(5)	-O(13)	2.2605(19)
	-O(11)	2.2841(18)		-O(10)	2.3146(18)
	-O(12)	2.324(2)		-O(12)	2.3920(18)
	-O(3)	2.3969(18)		-O(11)	2.408(2)
<Na(4)–O>		2.304		-O(6)	2.6694(18)
			<Na(5)–O>		2.409

been refined to 47 % and 42 %, respectively, for P(2) and P(2') (Table 9). This leads to the doubling of the *b* parameter (Fig. 6b).

There are ten large-cation sites occupied by Ag and Na statistically replacing each other, corresponding to the Na sites in the initial lomonosovite: two in the *O* sheet [*A*(1a) and *A*(1b)], two in the *H* sheet [*A*(2a) and *A*(2b)] and six in the interlayer space [*A*(3a-5b)]. The e_{ref} values found for these sites are: *A*(1a) - 29.1, *A*(1b) - 27.3, *A*(2a) - 14.4, *A*(2b) - 14.1, *A*(3a) - 14.9, *A*(3b) - 15.1, *A*(4a) - 36.1, *A*(4b) - 37.2, *A*(5a) - 29.0 and *A*(5b) - 30.1. The collected single-crystal X-ray diffraction data are an average between the initial lomonosovite and its Ag-exchanged form. Thus, the assignment of the multiple large-cation sites is clearly ambiguous. The obtained model of the crystal structure (a) confirms that Ag replaces Na and (b) shows preferable sites for Ag cations. Thus, sites *A*(4a) (average distance <*A*(4a)–O> 2.35 Å) and A(4b) (<*A*(4b)–O> 2.52/2.51 Å [calculated for polyhedra with bonds *A*(4b) –O(26)/ *A*(4b)–O(26'), respectively]) are Ag-dominant, *A*(1a) (<*A*(1a)–O> 2.51 Å), *A*(1b) (<*A*(1b)–O> 2.50 Å), *A*(5a) (<*A*(5a)–O> 2.44 Å) and *A*(5b) (<*A*(5b)–O> 2.48 Å; Table 10) are half-occupied by Ag, whereas positions in the *H* sheet *A*(2a) and *A*(2b) as well as the last two sites in the interlayer space, *A*(3a) and *A*(3b) are Na-dominant. Bond lengths <*A*–O> for the *A* sites, containing significant amount of Ag, are elongated as compared with the same sites in the initial lomonosovite. According to electron-microprobe data, sodium in the Ag-exchanged form of lomonosovite can be fully replaced by silver (Table 1), so it seems plausible that after the completion of the reaction Ag occupies all ten large cation sites, either solely or with a small admixture of Ca.

The P sites are partially vacant and we believe that ion exchange is accompanied by slight hydration with the replacement of the contact ion pairs ($Na^+ + PO_4^{3-}$) in the interlayer space by H_2O molecules according to the scheme: $3Na^+ + PO_4^{3-} \rightarrow xH_2O + \square$.

Bond-valence sums for fully occupied anion sites coordinating P(1), P(2) and P(2'), namely O(14), O(18), O(20), O(21), O(22), O(25), O(26) and O(26') are 1.84, 1.70, 1.73, 1,75, 1.85, 1.58 and 1.52 *vu*, respectively (Table 9). This indicates possible admixture of H_2O or OH^- which could occupy these sites when P sites are vacant. It can also be confirmed by the presence in the IR spectrum of the Ag-exchanged form of lomonosovite of weak absorption bands of O-H stretching vibrations (3443 cm^{-1}) and H-O-H bending vibrations: 1680 (shoulder), 1647 and 1544 cm^{-1} (Fig. 7). The presence of three non-degenerate bands of H-O-H bending vibrations in the IR spectrum indicates the presence of three locally nonequivalent H_2O molecules. There is no evidence of the presence of the PO_3OH groups in the IR spectrum (*i.e.* there are no absorption bands in the range from 1700 to 3000 cm^{-1}, Fig. 7), which excludes possible admixture of P–OH bonds.

It was initially supposed that the presence of bands corresponding to O-H stretching and H-O-H bending vibrations in the IR spectrum could be caused by admixture of murmanite formed after lomonosovite during the experiment. However, there are no reflections that could be assigned to murmanite in the X-ray powder-diffraction pattern of the Ag-exchanged form of lomonosovite, neither do reciprocal-space images reveal any contribution from a phase with the *c* unit-cell parameter close to that of murmanite, *i.e.* with $c \approx 12.2$ Å. Both patterns also show that no other layered titanosilicate with the *c* parameter distinctly different from one of a lomonosovite-like phase, *i.e.* with $c = 14.4$–14.5 Å, is present in the studied sample.

The other 18 anion sites, O(1–13, 15–17, 19, 24) are occupied solely by O^{2-}.

The formula of the Ag-exchanged form of lomonosovite obtained from the structural refinement is $\{Ag_{2.83}Na_{2.28}Ca_{0.20}\}$

Table 9. Atom coordinates (*x, y, z*), equivalent thermal displacement parameters (U_{eq}, Å^2), site occupancy factors (s.o.f.) and bond-valence sums (BVS) in the structure of the Ag-exchanged form of lomonosovite.

Atom	*x*	*y*	*z*	U_{eq}	s.o.f.[1]	BVS[3]
Si(1a)	0.1663(8)	0.0995(3)	0.1774(3)	0.0038(8)[2]	1	4.06
Si(1b)	0.1515(8)	0.3174(3)	0.1963(3)	0.0051(9)[2]	1	4.01
Si(2a)	0.8550(8)	0.1824(3)	0.8037(3)	0.0050(9)[2]	1	4.01
Si(2b)	0.8428(8)	0.4004(3)	0.8228(3)	0.0049(9)	1	4.06
P(1)	0.3261(8)	0.8926(3)	0.5710(3)	0.0076(16)	[13.2] 0.88(3)	4.20
P(2)	0.327(2)	0.3911(6)	0.5695(6)	0.008(3)[2]	[7.1] 0.47(3)	2.10
P(2')	0.217(3)	0.3944(7)	0.5738(7)	0.010(4)[2]	[6.3] 0.42(3)	1.90
Ti(1a)	0.3358(5)	0.03869(18)	0.78490(18)	0.0051(9)[2]	[23.6] $Ti_{0.91}Nb_{0.09}$	4.36
Ti(1b)	0.6645(5)	0.46118(18)	0.21474(18)	0.0053(9)[2]	[23.6] $Ti_{0.91}Nb_{0.09}$	4.36
Ti(2a)	0.2725(5)	0.1941(2)	0.99354(19)	0.0102(9)	[24.1] $Ti_{0.72}Mn_{0.20}Nb_{0.08}$	3.87
Ti(2b)	0.7336(5)	0.3058(2)	0.00605(19)	0.0102(9)	[23.9] $Ti_{0.73}Mn_{0.20}Nb_{0.07}$	3.85
A(1a)	0.7335(5)	0.05483(17)	0.0070(2)	0.0250(9)	[29.1] $Ag_{0.50}Na_{0.50}$	1.06
A(1b)	0.2694(5)	0.44504(18)	0.9959(2)	0.0260(10)	[27.4] $Na_{0.55}Ag_{0.45}$	0.98
A(2a)	0.6756(9)	0.2102(3)	0.2342(3)	0.0090(16)[2]	[14.4] $Na_{0.90}Ag_{0.10}$	1.10
A(2b)	0.3319(9)	0.2911(4)	0.7663(4)	0.0099(17)	[14.1] $Na_{0.91}Ag_{0.09}$	1.08
A(3a)	0.8218(11)	0.0169(4)	0.6418(4)	0.0168(19)	[14.9] $Na_{0.66}Ag_{0.12}Ca_{0.10}$	1.13
A(3b)	0.2021(13)	0.4825(4)	0.3583(4)	0.027(2)	[15.1] $Na_{0.67}Ag_{0.12}Ca_{0.10}$	1.22
A(4a)	0.1869(4)	0.23930(16)	0.39991(15)	0.0279(7)	[36.1] $Ag_{0.73}Na_{0.15}$	0.94
A(4b)	0.7657(6)	0.26026(17)	0.60037(17)	0.0422(10)	[37.2] $Ag_{0.76}Na_{0.13}$	0.96
A(5a)	0.2567(6)	0.1394(2)	0.5805(2)	0.0332(10)	[29.0] $Ag_{0.54}Na_{0.34}$	0.96
A(5b)	0.7130(6)	0.3611(2)	0.4198(2)	0.0332(10)	[30.1] $Ag_{0.56}Na_{0.33}$	0.85
O(1)	–0.075(2)	0.3693(8)	0.2468(9)	0.012(2)	1	1.94
O(2)	0.589(2)	0.2130(9)	0.0707(8)	0.012(2)	1	1.91
O(3)	0.081(3)	0.4456(10)	0.7912(10)	0.023(3)	1	2.03
O(4)	0.368(2)	0.0857(9)	0.9082(9)	0.015(3)	1	2.23
O(5)	0.636(2)	0.4145(10)	0.0915(9)	0.016(3)	1	2.17
O(6)	–0.056(2)	0.0456(9)	0.2098(9)	0.016(3)	1	2.06
O(7)	0.160(3)	0.2131(9)	0.2275(9)	0.016(3)	1	2.20
O(8)	0.820(2)	0.2865(9)	0.7726(9)	0.014(3)	1	2.20
O(9)	0.419(2)	0.2870(8)	0.9294(9)	0.012(2)	1	1.92
O(10)	0.863(2)	0.4013(9)	0.9342(9)	0.014(2)	1	2.08
O(11)	0.096(2)	0.3011(9)	0.0828(8)	0.012(2)	1	1.92
O(12)	–0.088(2)	0.1992(9)	0.9173(8)	0.012(2)	1	1.95
O(13)	0.089(2)	0.1373(8)	0.7522(8)	0.009(2)[2]	1	1.98
O(14)	0.711(3)	0.5107(9)	0.3668(9)	0.019(3)	1	1.84
O(15)	0.143(2)	0.0983(9)	0.0660(9)	0.014(2)	1	2.13
O(16)	0.409(3)	0.5516(10)	0.2134(10)	0.021(3)[2]	1	2.08
O(17)	0.607(2)	0.1233(8)	0.7578(8)	0.011(2)	1	1.93
O(18)	0.270(2)	–0.0110(9)	0.6337(9)	0.014(2)	1	1.70
O(19)	0.568(2)	–0.0606(9)	0.7862(9)	0.014(2)[2]	1	2.07
O(20)	0.755(3)	0.1934(9)	0.3875(10)	0.019(3)	1	1.73
O(21)	0.817(3)	0.3054(8)	0.5273(11)	0.028(3)	1	1.75
O(22)	0.283(4)	0.3052(9)	0.6126(10)	0.037(5)	1	1.85
O(23)	0.399(3)	0.1099(10)	0.4368(11)	0.024(3)	1	2.01
O(24)	0.410(2)	0.3695(9)	0.2425(9)	0.017(3)	1	1.91
O(25)	0.227(5)	0.3913(14)	0.4704(8)	0.076(9)	1	1.92
O(26)	0.606(3)	0.3900(18)	0.5598(19)	0.020(4)	[4.0] 0.50(3)	1.58[4]
O(26')	–0.067(4)	0.3903(18)	0.567(2)	0.020(4)	[4.0] 0.50(3)	1.52[4]

[1] Basing on the e_{ref} values (given in square brackets) and electron microprobe data we consider these occupancies of the sites, taking into account coordination polyhedra character and interatomic distances.
[2] U_{iso}.
[3] BVS have been formally calculated taking into account s.o.f.
[4] BVS to O(26) and O(26') are given as for full-occupied sites.

$\{Na_{1.05}Ag_{0.95}(Ti_{1.45}Mn_{0.20}Nb_{0.15})^{2}\}\{Na_{1.81}Ag_{0.19}(Ti_{1.82}Nb_{0.18})[Si_2O_7]_2\}O_2(PO_4)_{1.77}(H_2O)_x$, in which the contents of the interlayer space, *O* and *H* sheets are correspondingly given in braces.

[2]This site can also contain minor admixture of Fe^{3+}.

Cu-exchanged lomonosovite

The Cu-exchanged form of lomonosovite is characterized by significantly decreased unit-cell parameter c = 13.969(5) Å as compared to the initial lomonosovite: 14.4871(4) Å (Table 2). The topology of the *HOH*

Table 10. Selected interatomic distances (Å) for the Ag-exchanged form of lomonosovite.

Ti(1a)-octahedron			Ti(1b)-octahedron			Ti(2a)-octahedron			Ti(2b)-octahedron		
Ti(1a)	-O(4)	1.806(14)	Ti(1b)	-O(5)	1.806(14)	Ti(2a)	-O(4)	1.931(14)	Ti(2b)	-O(9)	1.926(13)
	-O(19)	1.898(13)		-O(16)	1.895(15)		-O(2)	1.936(13)		-O(5)	1.937(14)
	-O(6)	1.944(13)		-O(3)	1.927(14)		-O(9)	1.953(12)		-O(2)	1.954(12)
	-O(17)	2.005(13)		-O(1)	2.002(12)		-O(15)	2.026(13)		-O(10)	2.017(13)
	-O(13)	2.023(12)		-O(24)	2.010(13)		-O(11)	2.137(13)		-O(12)	2.138(13)
	-O(18)	2.197(13)		-O(14)	2.207(14)		-O(12)	2.145(12)		-O(11)	2.160(12)
<Ti(1a)–O>		1.98	<Ti(1b)–O>		1.98	<Ti(2a)–O>		2.02	<Ti(2b)–O>		2.03
Si(1a)-tetrahedron			Si(1b)-tetrahedron			Si(2a)-tetrahedron			Si(2b)-tetrahedron		
Si(1a)	-O(6)	1.576(13)	Si(1b)	-O(24)	1.606(13)	Si(2a)	-O(17)	1.603(12)	Si(2b)	-O(3)	1.581(14)
	-O(19)	1.614(13)		-O(1)	1.617(13)		-O(13)	1.625(12)		-O(16)	1.608(15)
	-O(15)	1.617(13)		-O(7)	1.627(13)		-O(8)	1.630(12)		-O(10)	1.619(13)
	-O(7)	1.667(13)		-O(11)	1.631(13)		-O(12)	1.634(13)		-O(8)	1.666(13)
<Si(1a)–O>		1.62	<Si(1b)–O>		1.62	<Si(2A)–O>		1.62	<Si(2b)–O>		1.62
P(1)-tetrahedron			P(2)-tetrahedron			P(2')-tetrahedron					
P(1)	-O(23)	1.504(16)	P(2)	-O(25)	1.491(9)	P(2')	-O(22)	1.504(12)			
	-O(20)	1.537(13)		-O(22)	1.493(9)		-O(14)	1.507(16)			
	-O(21)	1.553(16)		-O(14)	1.532(17)		-O(25)	1.512(14)			
	-O(18)	1.573(13)		-O(26)	1.575(16)		-O(26')	1.530(17)			
<P(1)–O>		1.54	<P(2)–O>		1.52	<P(2')–O>		1.51			
A(1a)-octahedron			*A*(1b)-octahedron			*A*(2a)-polyhedron			*A*(2b)-polyhedron		
A(1a)	-O(15)	2.330(13)	*A*(1b)	-O(10)	2.320(13)	*A*(2a)	-O(20)	2.290(15)	*A*(2b)	-O(22)	2.279(15)
	-O(15)	2.400(13)		-O(5)	2.389(13)		-O(2)	2.393(13)		-O(9)	2.391(14)
	-O(4)	2.409(13)		-O(10)	2.412(14)		-O(19)	2.458(14)		-O(13)	2.515(13)
	-O(2)	2.460(13)		-O(9)	2.481(12)		-O(1)	2.602(13)		-O(3)	2.591(16)
	-O(4)	2.609(13)		-O(5)	2.621(13)		-O(7)	2.633(15)		-O(16)	2.595(15)
	-O(12)	2.837(12)		-O(11)	2.796(12)		-O(24)	2.688(14)		-O(8)	2.635(14)
<*A*(1a)–O>		2.51	<*A*(1b)–O>		2.50		-O(6)	2.762(14)		-O(8)	2.778(14)
							-O(7)	2.778(15)		-O(17)	2.816(13)
						<*A*(2a)–O>		2.58	<*A*(2b)–O>		2.57
A(3a)-polyhedron			*A*(3b)-polyhedron			*A*(4a)-polyhedron			*A*(4b)-polyhedron		
A(3a)	-O(23)	2.238(15)	*A*(3b)	-O(26)	2.13(3)	*A*(4a)	-O(25)	2.241(19)	*A*(4b)	-O(26)	2.19(2)
	-O(21)	2.301(16)		-O(26')	2.19(3)		-O(23)	2.287(14)		-O(26')	2.21(2)
	-O(18)	2.471(14)		-O(25)	2.249(16)		-O(20)	2.399(14)		-O(21)	2.263(15)
	-O(17)	2.477(13)		-O(1)	2.467(13)		-O(7)	2.476(13)		-O(8)	2.470(13)
	-O(13)	2.490(13)		-O(24)	2.502(15)	<*A*(4a)–O>		2.35		-O(22)	2.71(2)
	-O(6)	2.677(15)		-O(14)	2.704(16)					-O(22)	2.85(2)
<*A*(3a)–O>		2.44		-O(14)	2.762(16)				<*A*(4b)–O>		2.52/2.51[1]
				-O(16)	2.811(16)						
			<*A*(3b)–O>		2.52/2.53[1]						
A(5a)-polyhedron			*A*(5b)-polyhedron								
A(5a)	-O(23)	2.290(16)	*A*(5b)	-O(26)	2.16(3)						
	-O(22)	2.337(12)		-O(26')	2.32(3)						
	-O(18)	2.397(13)		-O(20)	2.377(13)						
	-O(21)	2.432(17)		-O(14)	2.386(14)						
	-O(13)	2.763(12)		-O(25)	2.81(3)						
<*A*(5a)–O>		2.44		-O(25)	2.82(3)						
			<*A*(5b)–O>		2.48						

[1] Calculated for polyhedra with bonds *M*- O(26)/*M* - O(26')

block remains unchanged. There are two Na-dominant sites in the Cu-exchanged form of lomonosovite: Na(o) in the *O*-sheet corresponding to the Na(1) site in the initial lomonosovite and Na(i) in the interlayer space as a superposition of the vacant Na(2) site in the *H* sheet and Na(4) and Na(5) sites in the interlayer space of the

Table 11. Atom coordinates (*x, y, z*), equivalent thermal displacement parameters (U_{eq}, Å^2), site occupancy factors (s.o.f.) and bond-valence sums (BVS) in the structure of the Cu-exchanged form of lomonosovite.

Atom	*x*	*y*	*z*	U_{eq}	s.o.f.[1]	BVS[6]
Si(1)	0.6541(9)	0.6326(7)	0.2069(3)	0.0192(11)	1	4.08
Si(2)	0.7016(10)	0.2115(7)	0.1941(3)	0.0232(12)	1	4.09
Ti(1)	0.1822(5)	0.9272(4)	0.2217(2)	0.0152(8)	1	4.23
Ti(2)	0.2486(5)	0.6230(4)	0.00468(19)	0.0199(11)	[24.4] $Ti_{0.62}Mn_{0.30}Nb_{0.08}$	4.03
P	0.1751(17)	0.1905(10)	0.4453(5)	0.029(3)	[10.2] 0.68(3)	*3.30*[8]
P'	0.3265[3]	0.1936[3]	0.447[3]	0.009(7)[2]	[3.2] 0.21(3)	*1.08*[8]
Cu(1)	0.6809(6)	0.9642(4)	0.3584(2)	0.0263(11)	[22.9] 0.785(13)	1.37
Cu(2)[4]	0.5	1	0	0.022(6)[2]	[4.4] 0.10[5]	0.14
Na(o)	0.803(2)	0.889(2)	–0.0117(12)	0.056(7)	[6.5] 0.59(4)	0.52
Na(i)	0.789(2)	0.3233(11)	0.6011(6)	0.044(3)	[11.2] $Na_{0.65}Ca_{0.20}$	1.05
O(1)	0.167(2)	0.8353(18)	0.0906(6)	0.025(3)	1	2.17
O(2) = (O,OH)	0.087(2)	0.4256(18)	0.0695(9)	0.025(3)	1	1.56
O(3)	0.704(3)	0.4362(19)	0.2437(9)	0.029(3)	1	2.17
O(4)	0.409(2)	0.4042(17)	–0.0869(8)	0.021(3)	1	2.06
O(5)	0.367(3)	0.7896(15)	–0.0800(9)	0.036(3)	1	1.97
O(6)	0.425(3)	0.731(2)	0.2598(10)	0.037(4)	1	1.90
O(7)	–0.093(3)	0.7717(19)	0.2476(9)	0.030(3)	1	2.03
O(8)	0.519(3)	0.083(2)	0.242(1)	0.036(3)	1	1.75
O(9)	–0.002(3)	0.1499(19)	0.2178(11)	0.037(3)	1	1.92
O(10)	0.228(3)	0.0098(18)	0.3811(9)	0.034(3)	1	1.83
O(11)	0.274(3)	0.217(2)	0.5518(9)	0.044(4)	1	1.70
O(12)	0.241(3)	0.364(2)	0.4036(12)	0.052(4)	1	1.43
O(13)	–0.119(5)	0.180(4)	0.4407(18)	0.049(6)	[5.6] 0.69[5]	1.36[7]
O(13')	0.616(4)	0.182(6)	0.450(3)	0.035(16)[2]	[2.6] 0.32(5)	1.50[7]

[1] Basing on the e_{ref} values (given in square brackets) and electron microprobe data we consider these occupancies of the sites, taking into account coordination polyhedra character and interatomic distances.
[2] U_{iso}.
[3] Atom coordinates of the P' site are fixed
[4] Multiplicities of the Cu(2) is 1, multiplicities of all other sites are 2.
[5] Values were fixed on the last stages of the refinement.
[6] BVS have been formally calculated taking into account s.o.f.
[7] BVS to O(13) and O(13') are given as for full-occupied sites
[8] See the text

initial lomonosovite (Fig. 5b). The Na(i) site contains Na, Ca and vacancies (e_{ref} = 11.2) whereas Na(o) hosts Na and vacancies (e_{ref} = 6.5, Table 11). The Cu^{2+} cations occupy two crystallographically independent positions. The Cu(1) site, corresponding to the Na(3) site in the initial lomonosovite, is located in a cavity in the interlayer space under the square window in the *H* sheet. It is occupied solely by Cu^{2+} (79 % of site occupancy) with the average <Cu(1)–O> distance of 2.18/2.17 Å [calculated for polyhedra with the bonds Cu(1)–O(13)/Cu(1)–O(13'), respectively]. The low-occupancy Cu(2) site is located in the inversion centre in the *O* sheet; this site is vacant in the initial lomonosovite. The Cu(2) cation is surrounded by six O atoms forming an octahedron distorted due to the Jahn-Teller effect. It has four short Cu–O distances [two of 1.778(9) and two of 1.816(9) Å] and two elongated Cu–O(1) bonds of 2.640(12) Å (Table 12). Sodium in the Na(o) position has to be partially substituted for O which is a ligand to a Cu(2) site (Fig. 8) and the Cu(2) site hosts Cu only when the Na(1) site is occupied by O.

The Cu-exchanged form of lomonosovite demonstrates a splitting of the P site along *a* into the two subsites P and P'. The occupancies have been refined to 68 % (P) and 21 % (P'), respectively. Thus PO_4 tetrahedra have two possible orientations, with splitting of one apical site into two subsites: O(13) and O(13') with the occupancies 69 and 32 % for PO_4- and P'O_4-tetrahedra, respectively.

The total site occupancy factor for P sites shows that ion exchange is accompanied by a slight hydration according to the scheme $3Na^+ + PO_4^{3-} \rightarrow xH_2O + \square$, the same as in the case of the Ag-exchanged form of lomonosovite. The bond-valence sums for anion sites coordinating the P and P', namely O(10), O(11), O(12), O(13) and O(13') are 1.83, 1.70, 1.43, 1.36 and 1.50 *vu*, respectively (Table 11). This indicates the admixture of H_2O or OH^- which could occupy these sites when P and P' sites are vacant, as in the Ag-exchanged form of lomonosovite. It is confirmed by the appearance of absorption bands of O-H stretching vibrations (at 3220 and 3440 cm^{-1}) and H-O-H bending vibrations (at 1650 cm^{-1}; Fig. 7) in the IR spectrum of the Cu-exchanged form of lomonosovite. Like the previous case, there is no evidence of the presence of PO_3OH groups.

Some positive charge deficiency in the *HOH* block caused by leaching of Na from both *O* and *H* sheets is

Table 12. Selected interatomic distances (Å) for Cu-exchanged form of lomonosovite.

Ti(1) - octahedron			Ti(2) - octahedron		
Ti(1)	-O(1)	1.827(8)	Ti(2)	-O(1)	1.860(11)
	-O(9)	1.898(14)		-O(2)	1.926(12)
	-O(7)	1.903(13)		-O(5)	1.957(14)
	-O(6)	2.025(13)		-O(2)	2.022(13)
	-O(8)	2.028(16)		-O(4)	2.054(12)
	-O(10)	2.184(13)		-O(4)	2.108(12)
<Ti(1)–O>		1.98	<Ti(2)–O>		1.99
Si(1) - tetrahedron			Si(2) - tetrahedron		
Si(1)	-O(3)	1.598(15)	Si(2)	-O(8)	1.587(16)
	-O(7)	1.608(14)		-O(3)	1.590(13)
	-O(6)	1.620(13)		-O(9)	1.635(13)
	-O(4)	1.641(12)		-O(5)	1.647(15)
<Si(1)–O>		1.62	<Si(1)–O>		1.62
P - tetrahedron			P' - tetrahedron		
P	-O(10)	1.493(14)	P'	-O(11)	1.504(12)
	-O(11)	1.493(14)		-O(10)	1.505(12)
	-O(12)	1.507(17)		-O(12)	1.512(13)
	-O(13)	1.54(3)		-O(13')	1.527(19)
<P–O>		1.51	<P'–O>		1.51
Na(o) - octahedron			Na(i) - polyhedron		
Na(o)	-O(1)	2.337(17)	Na(i)	-O(13')	2.24(4)
	-O(2)	2.369(19)		-O(12)	2.259(16)
	-O(5)	2.409(19)		-O(13)	2.41(2)
	-O(1)	2.43(2)		-O(10)	2.439(16)
	-O(5)	2.667(18)		-O(6)	2.439(17)
	-O(4)	2.96(2)		-O(7)	2.695(16)
<Na(o)–O>		2.53		-O(11)	2.76(2)
				-O(11)	2.816(19)
			<Na(i)–O>		2.55/2.52[1]
Cu(1) - octahedron			Cu(2) - octahedron		
Cu(1)	- O(13')	1.91(4)	Cu(2)	- O(5)	1.778(9) × 2
	- O(13)	1.95(3)		-Na(o)	1.816(9) × 2
	-O(11)	1.959(15)		-O(1)	2.640(12) × 2
	-O(8)	2.072(14)	<Cu(1)–O>		2.08
	-O(6)	2.260(16)			
	-O(7)	2.348(14)			
	-O(10)	2.470(15)			
<Cu(1)–O>		2.18/2.17[1]			

[1] Calculated for polyhedra with bonds *M*- O(13)/*M* - O(13')

compensated by partial protonation of the Ti(2)-O-Ti(2) bridge oxygen O(2). The bond-valence sum for O(2) is 1.56 *vu*. It is confirmed by the appearance of absorption bands at 3491 and 3575 cm^{-1} in the IR spectrum of the Cu-exchanged form of lomonosovite, corresponding to O-H stretching vibrations of basic OH groups (Fig. 7).

The formula of the Cu-exchanged form of lomonosovite obtained from the structural refinement is $\{Cu_{1.58}Na_{1.30}Ca_{0.40}\}\{Na_{1.04}Cu_{0.1}(Ti_{1.24}Mn_{0.60}Nb_{0.16})\}\{Ti_{2.00}[Si_2O_7]_2\}O_2(O,OH)_2(PO_4)_{1.78}(H_2O)_x$, in which the contents of the interlayer space, *O* and *H* sheets are correspondingly given in braces. It is in agreement with the electron microprobe data (Table 1).

Conclusions

Murmanite and lomonosovite show strong ion-exchange capacity for chalcophile elements, Ag and Cu. These cations can occupy the positions in the interlayer space, *O* and *H* sheets whereas the general topology of the main

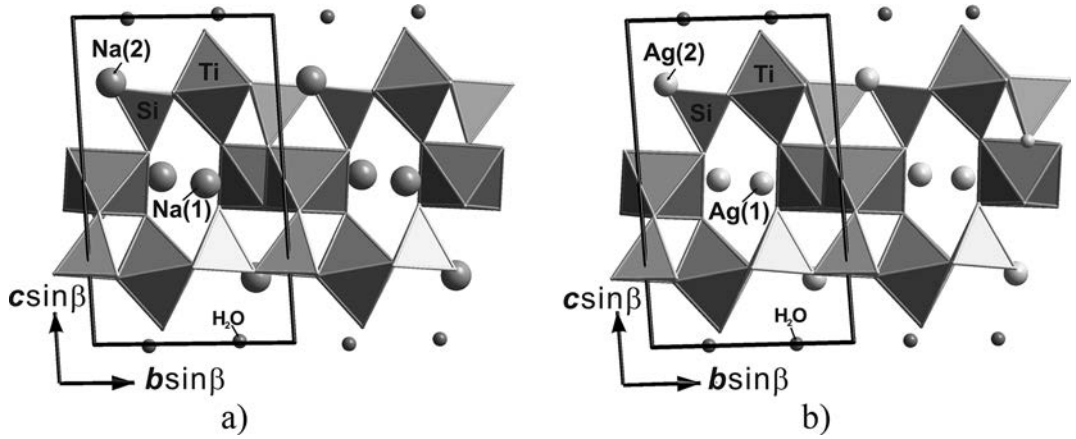

Fig. 3. The crystal structure of murmanite (a) and its Ag-exchanged form (b) projected along *a*. The unit cells are outlined.

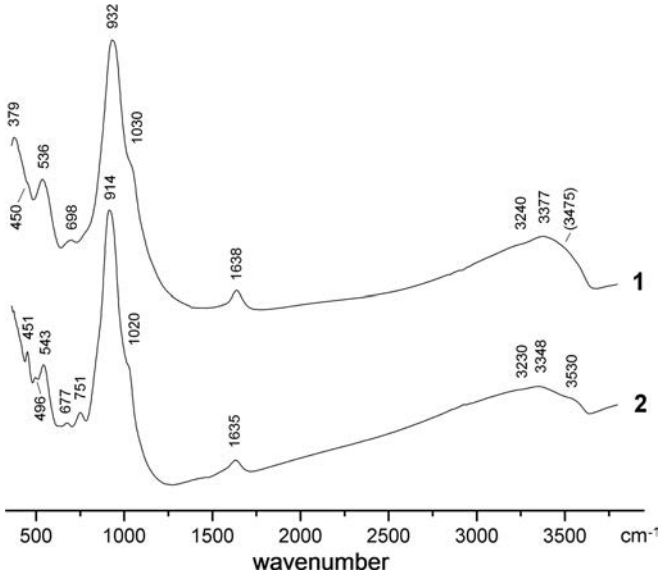

Fig. 4. IR spectra of murmanite (1) and the product of its ion exchange with 1N $AgNO_3$ solution at 90°C during 5 hours (2).

heteropolyhedral *HOH* block remains unchanged in all cases. This allows us to consider the heterophyllosilicates murmanite and lomonosovite as natural microporous materials that are cation exchangers with mobile Na cations in both the interlayer space (a 2D system of channels) and the *HOH* block. As their combination, a 3D system of channels appears.

In both compounds Ag^+ replaces Na^+ or fills vacancies at all large cation sites. The Cu^{2+} cations in the Cu-exchanged form of lomonosovite occupy one site in the interlayer space, corresponding to one of the three Na sites in the initial lomonosovite, and one low-occupancy site in the *O* sheet (on the inversion centre). The latter site centers an octahedron with Jahn-Teller elongation, as for many other Cu^{2+} compounds. The exchange of Na^+ for Cu^{2+} is accompanied by leaching of Na from the two other sites in the interlayer space of lomonosovite to form a cation-deficient phase with vacancies in all large-cation sites. The Ca^{2+} ion, partially substituting Na^+ in the initial murmanite and lomonosovite, is rigidly fixed in their structures and is almost inert during the exchange.

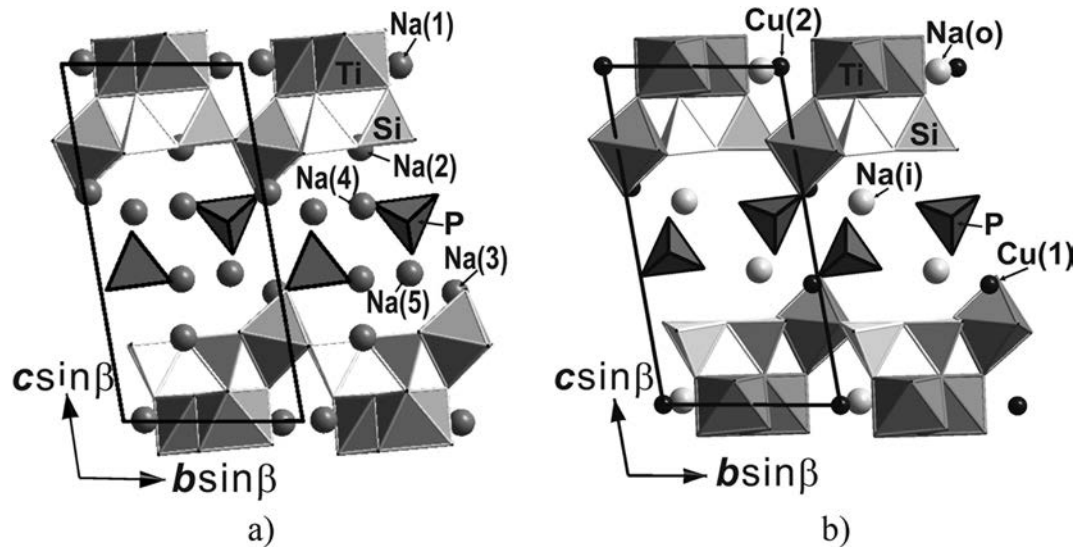

Fig. 5. The crystal structure of lomonosovite (a) and its Cu-exchanged form (b) projected along *a*. Large-cation sites are shown as circles. The unit cells are outlined

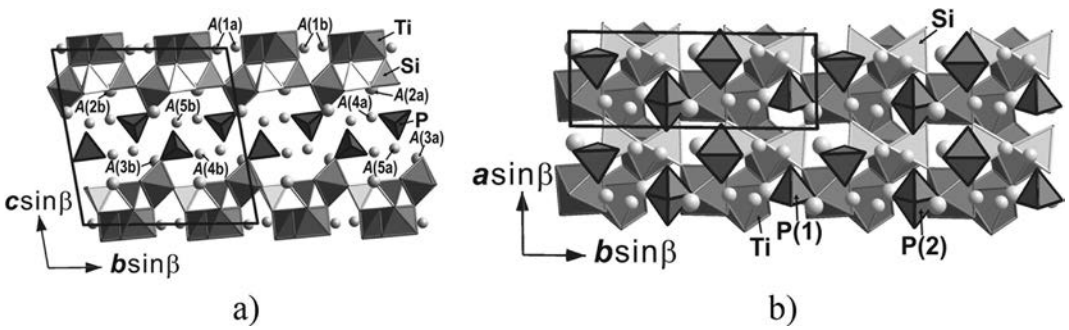

Fig. 6. The crystal structure of the Ag-exchanged form of lomonosovite projected along *a* (a) and *c* (b). Large-cation sites are shown as circles. The unit cell is outlined.

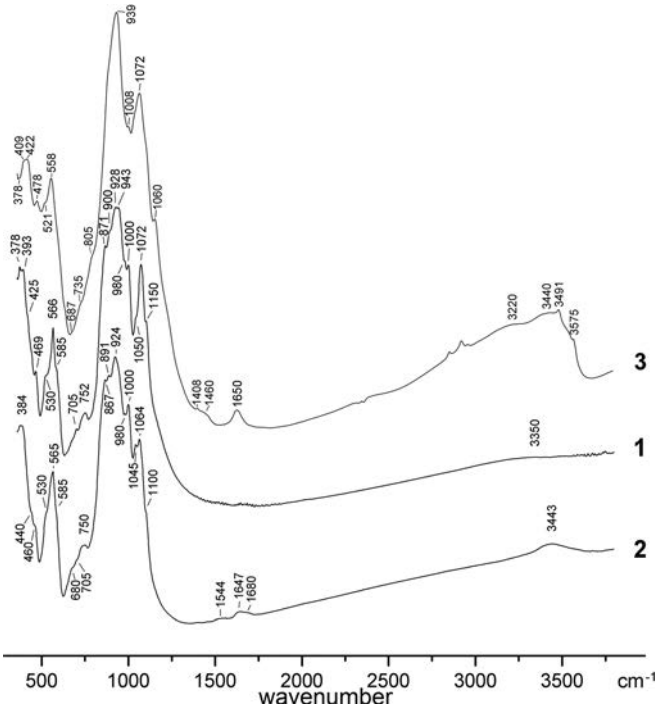

Fig. 7. IR spectra of lomonosovite (1), the product of its ion exchange with 1N $AgNO_3$ solution during 72 hours (2) and with 1N $CuSO_4$ solution during 28 hours (3) at 150°C.

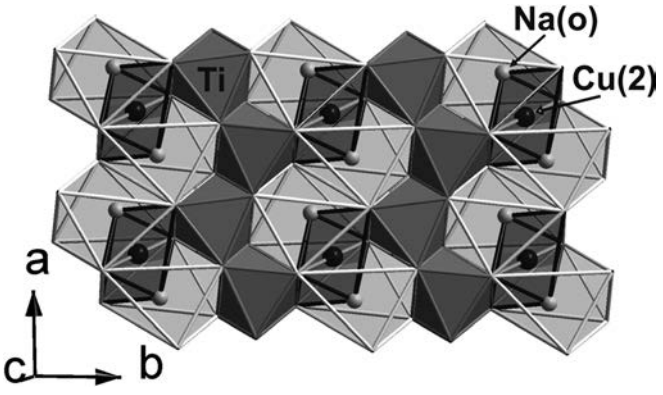

Fig. 8. The *O* sheet in the crystal structure of the Cu-exchanged form of lomonosovite.

Charge deficiency of cation-exchanged phases (caused by filling vacancies by Ag^+ or, in case of the reaction with Cu^{2+}, leaching of Na^+) is compensated by protonation/deprotonation of the bridging O atom in Ti-O-Ti.

Ion-exchange in the PO_4-bearing heterophyllosilicate lomonosovite is accompanied by its slight hydration according to the scheme $3Na^+ + PO_4^{3-} \rightarrow xH_2O + \square$.

Ion exchange in lomonosovite results in the splitting of the P site in the interlayer space to form two P sites, statistically occupying two tetrahedra with 50 % occupancy. There are two crystallographically nonequivalent P positions in the Ag-exchanged form of lomonosovite instead of one site in the initial lomonosovite. Additionally, one of these sites is split that causes doubling of the *b* parameter and, consequently, the unit-cell volume. Splitting of both or only of the P sites in the interlayer space is clearly dependent on the type of exchangable cation, but the cause of it is still the subject of further examination.

Acknowledgements: We are grateful to Gerald Giester for his help in XRD data collection and Olga V. Yakubovich for fruitful discussion. We thank Péter Németh and anonymous referee for their valuable comments and Sergey V. Krivovichev for his editorial work. This work was supported by Russian Foundation for Basic Research, grants nos. 12-05-90831-mol_rf_nr, 12-05-31212-mol_a, 13-05-12021_ofi_m and 14-05-00190-a, and by the Foundation of the President of the Russian Federation, grants nos. NSh-1130.2014.5 and MD-2088.2014.5. The support by the SPbSU X-Ray Diffraction Resource Center is acknowledged.

References

Belov, N.V., Gavrilova, G.S., Solov'eva, L.P., Khalilov, A.D (1977): The refined structure of lomonosovite. *Sov. Phys. Dokl.*, **235**, 1064–1067. (in Russian)

Borneman-Starynkevich, I.D (1946): On chemical nature of murmanite. *in* ''Problems of Mineralogy, Geochemistry and Petrography'' (Ed. D.S. Belyankin), AN USSR, Moscow-Leningrad, 66–74. (in Russian)

Brese, N.E. & O'Keeffe, N.E (1991): Bond-valence parameters for solids. *Acta Crystallogr.*, **47**, 192–197.

Cámara, F., Sokolova, E., Hawthorne, F.C., Abdu, Y (2008): From structure topology to chemical composition. IX. Titanium silicates: revision of the crystal chemistry of lomonosovite and murmanite, Group-IV minerals. *Mineral. Mag.*, **72**, 1207–1228.

Chukanov, N.V. & Pekov, I.V (2005): Heterosilicates with tetrahedral-octahedral frameworks: mineralogical and crystal-chemical aspects. *Rev. Mineral. Geochem.*, **57**, 105–143.

Ferraris, G. & Gula, A (2005): Polysomatic aspects of microporous minerals – heterophyllosilicates, palysepioles and rhodesite-related structures. *Rev. Mineral. Geochem.*, **57**, 69–104.

Gerasimovsky, V.I. (1945): Mineralogy of the Lovozero Alkaline Massif. Dr. Sci. thesis. Moscow, 258 p. (in Russian).

— (1950): Lomonosovite, a new mineral. *Dokl. Akad. Nauk SSSR*, **70**, 83–86. (in Russian)

Gutkova, N.N (1930): A new titano-silicate – murmanite from Lovozero tundras. *Dokl. Akad. Nauk SSSR*, ser. A, **27**, 731–736. (in Russian)

Khalilov, A.D (1989): The refinement of murmanite crystal structure and new data on its crystallo-chemical features. *Mineral. J.*, **11**, 19–27. (in Russian)

Khalilov, A.D., Makarov, E.S., Mamedov, Kh., P'yanzina, S, Ya, L (1965): On the crystal structure of minerals of the murmanite-lomonosovite group. *Dokl. Akad. Nauk SSSR*, **162**, 179–182. (in Russian)

Khomyakov, A.P (1995): Mineralogy of hyperagpaitic alkaline rocks. Clarendon Press, Oxford, 223 p.

Lykova, I.S., Chukanov, N.V., Tarasov, V.P., Pekov, I.V., Yapaskurt, V.O (2013a): Ion exchange properties of murmanite $Na_2Ti_2(Si_2O_7)O_2 \cdot 2H_2O$. *Russ. J. Phys. Chem. B Focus Phys.*, **32**, 35–42. (in Russian)

Lykova, I.S., Chukanov, N.V., Kazakov, A.I., Tarasov, V.P., Pekov, I.V., Yapaskurt, V.O., Chervonnaya, N.A (2013b): Murmanite and lomonosovite as Ag-selective ionites: kinetics and products of ion exchange in aqueous $AgNO_3$ solutions. *Phys. Chem. Minerals*, **40**, 625–633.

Németh, P., Ferraris, G., Radnóczi, G., Ageeva, O.A (2005): TEM and X-ray study of syntactic intergrowths of epistolite, murmanite and shkatulkalite. *Can. Mineral.*, **43**, 973–998.

Pekov, I.V. & Chukanov, N.V (2005): Microporous framework silicate minerals with rare and transition elements: minerogenetic aspects. *Rev. Mineral. Geochem.*, **57**, 145–171.

Ramsay, W (1890): Geologische Beobachtungen auf der Halbinsel Kola. Nebst einem Anhange: Petrographische Beschreibung der Gesteine des Lujavr-urt. *Fennia*, **3**, 1–52.

Rastsvetaeva, R.K. & Andrianov, V.N (1986): New data on the crystal structure of murmanite. *Kristallografiya*, **31**, 82–87. (in Russian)

Rastsvetaeva, R.K., Simonov, V.I., Belov, N.V (1971): The crystal structure of lomonosovite. *Dokl. Akad. Nauk SSSR*, **197**, 81–84. (in Russian)

Selivanova, E.A. (2012): The exchange processes and evolution of titanosilicates in the Kibiny and Lovozeto alkaline massifs. Dissertation, Saint-Petersburg State University (in Russian).

Sheldrick, G.M (2008): A short history of SHELX. *Acta Crystallogr.*, **A64**, 112–122.

Received 29 August 2014
Modified version received 22 January 2015
Accepted 26 February 2015